Friction Torque Dynamics Associated with Intraseasonal Length-of-Day Variability

STEVEN B. FELDSTEIN

EMS Environmental Institute, The Pennsylvania State University, University Park, Pennsylvania

(Manuscript received 26 June 2000, in final form 23 March 2001)

ABSTRACT

This investigation examines the dynamical processes that drive the anomalous friction torque associated with intraseasonal length-of-day fluctuations. Diagnostic analyses with National Centers for Environmental Protection–National Center for Atmospheric Research reanalysis and National Oceanic and Atmospheric Administration outgoing longwave radiation data are performed. The approach adopted is to use the mean meridional circulation (MMC) as a proxy for the friction torque, and then to examine the MMC that is driven both by eddy fluxes and zonal mean diabatic heating.

The following simple picture emerges from this analyses. For the austral winter (May through September), the anomalous friction torque in both hemispheres is driven by anomalous zonal mean convection. For the boreal winter (November through March), the anomalous friction torque in the Northern Hemisphere is driven primarily by eddy fluxes, whereas in the Southern Hemisphere the anomalous friction torque is also driven by anomalous zonal mean convection. However, the dynamics associated with this convection for the Southern Hemisphere boreal winter may be rather subtle, as the results suggest that this convection may in turn be driven by eddies within the Northern Hemisphere.

1. Introduction

Several recent papers have addressed the question of what dynamical processes drive the anomalous friction torque associated with intraseasonal length-of-day (LOD) and global atmospheric angular momentum (GAAM) variability. One mechanism that has been proposed for generating anomalous friction torques involves fluctuations in the zonally averaged mean meridional circulation (MMC). The influence of the zonally averaged Coriolis force on the low-level meridional winds of the anomalous MMC results in an acceleration of the low-level zonally averaged zonal wind, and hence an anomalous friction torque. These changes in the MMC, which arise from the flow adjusting to thermal wind balance, can be driven by anomalous eddy heat and eddy angular momentum fluxes, and other mechanical and thermodynamic processes, such as friction and diabatic heating, respectively. Two particular studies have presented results which are consistent with this mechanism of friction torque generation for intraseasonal timescales. Weickmann and Sardeshmukh (1994) showed that during the boreal winter, in the Northern Hemisphere (NH), the zonally and vertically integrated eddy angular momentum flux convergence has a temporal and spatial pattern that is consistent with the anomalous friction torque being generated by the inducement of an anomalous eddy-driven MMC. In addition, Hendon (1995) showed that the spatial and temporal pattern of the zonally averaged outgoing longwave radiation (OLR) and meridional wind fields are consistent with an anomalous friction torque being driven by an anomalous MMC associated with fluctuations in zonal mean tropical diabatic heating.

Further support for the role of the MMC in driving the intraseasonal friction torque was provided by Feldstein (1999). This was accomplished by separating the anomalous friction torque (note that the friction torque is a nonlinear quantity) into two components, one involving the product of zonal mean quantities, and the other involving the product of eddy (deviation from zonal mean) quantities. He was able to show with the National Centers for Environmental Prediction (NCEP)–National Center for Atmospheric Research (NCAR) reanalysis data that the zonal mean contribution to the anomalous friction torque was overwhelmingly dominant. This was the case both for the austral winter [see Fig. 11 in Feldstein (1999)] and the boreal winter (see conclusions in that paper). Furthermore, Feldstein (1999) also showed that the angular momentum budget at the lowest level in the reanalysis model is dominated by a balance between the anomalous Coriolis and frictional forces. The implication of these results, together with the above property that the zonal mean contribution to the anomalous friction torque is dominant, is that the anomalous friction torque asso-

Corresponding author address: Dr. Steven B. Feldstein, 2217 Earth-Engineering Science Building, EMS Environmental Institute, The Pennsylvania State University, University Park, PA 16802.
E-mail: sbf@essc.psu.edu

© 2001 American Meteorological Society

Unauthenticated | Downloaded 05/11/21 11:37 AM UTC

ciated with intraseasonal LOD fluctuations is indeed primarily driven by fluctuations in the anomalous MMC.

The goal of this study is to test the theories proposed by Weickmann and Sardeshmukh (1994) and Hendon (1995) that the anomalous friction torque associated with intraseasonal LOD variability is driven by eddy fluxes and zonal mean tropical diabatic heating, respectively. The test will be performed by first calculating the anomalous MMC driven by both eddy fluxes and zonal mean diabatic heating, and then by comparing the results with the anomalous observed MMC. The anomalous MMC, rather than the anomalous friction torque, is used because while it is not at all apparent how one would calculate the anomalous eddy-driven friction torque, the use of the omega equation allows for straightforward calculation of an anomalous eddy-driven MMC. Of course, it is the balance between the Coriolis and frictional forces, as described in the above paragraph, that allows us to use the anomalous MMC as a proxy measure of the anomalous friction torque. However, it is important to emphasize that this approach can only yield qualitative, not quantitative, results. This is primarily because of various approximations used in both the omega equation and the diabatic heating field. Nevertheless, we believe that the results of this study do add much insight into the dynamics of the intraseasonal friction torque.

The data and methodology are presented in section 2. The results are shown in section 3, followed by the conclusions in section 4.

2. Data and methodology

Most quantities analyzed in this study are derived from daily NCEP–NCAR reanalysis data extending from 1 January 1979 to 31 December 1995. These quantities include the friction torque, and the eddy momentum and heat fluxes. Additional quantities are the OLR field, which is produced by the National Oceanic and Atmospheric Administration (NOAA), and is used as a proxy for tropical convection, and the LOD time series, which was kindly provided by P. Nelson of Atmospheric and Environmental Research, Inc. The data are examined separately for the boreal winter and austral winter seasons, defined as November through March, and May through September, respectively.

The friction torque is expressed as

$$T_F(\theta) = a^2 \cos^2\theta \int_0^{2\pi} \tau_s \, d\lambda, \qquad (1)$$

where τ_s is the surface viscous stress and is defined to be positive when angular momentum is transfered from the solid earth to the atmosphere, a is the earth's radius, and θ and λ are latitude and longitude, respectively.

The observed anomalous mass streamfunction is calculated from the observed anomalous zonally averaged meridional wind by integrating the zonally averaged continuity equation downward from the top of the atmosphere. This calculation assumes a zero vertical velocity at the top of the atmosphere (see Peixoto and Oort 1992).

Except for the OLR field, all other quantities in this study are generated from data at rhomboidal 30 horizontal resolution. The horizontal resolution of the OLR field is 2.5° lat × 2.5° long. For the vertical resolution, all 28 of the reanalysis model's sigma levels are retained. These levels range from $\sigma = 0.995$ to $\sigma = 0.0027$.

In order that our analysis encompasses the range of periods associated with statistically significant spectral peaks in the LOD time series, which form a broad band of periods near 50 days, (e.g., Langley et al. 1981; Rosen and Salstein 1983; Lau et al. 1989; Dickey et al. 1991; Magana 1993), a 30–70-day bandpass filter is applied to all quantities in this study. For quantities such as the eddy heat and momentum fluxes, this filter is applied to the covariance, and not the individual wind and temperature fields that comprise the flux. Furthermore, unless stated otherwise, all quantities are presented as linear regressions against the LOD tendency time series.[1] For each of these calculations, the amplitude of the LOD tendency is one standard deviation.

In order to estimate the MMC response to the driving by the anomalous eddy momentum and heat fluxes, we follow the approach used by Haynes and Shepherd (1989) to solve the omega equation (see their paper for complete detail). Although the use of this technique involves the approximations inherent with quasigeostrophic diagnostics, the findings of Kim and Lee (2001a,b) suggest that this approximation can indeed be very useful. For example, in their examination of the Hadley cell in a multilevel primitive equation model, for realistic parameter settings, they find a difference on the order of 10%–20% between the model's Hadley cell and the Hadley cell derived from the omega equation. It is only for their two-dimensional axisymmetric calculations when the zonally averaged meridional temperature gradient is unrealistically large that they find large errors with the omega equation. The omega equation can be written symbolically as

$$L\omega(p, \mu) = F^M + F^H + D + Q, \qquad (2)$$

where

$$L = \frac{\partial}{\partial\mu}\left[\frac{(1-\mu^2)}{\mu^2}\frac{\partial}{\partial\mu}\right] + \frac{4\Omega^2 a^2 p}{R\Gamma}\frac{\partial^2}{\partial p^2}, \qquad (3)$$

$\mu = \sin(\theta)$, Ω is the earth's angular velocity, p is the pressure, R is the gas constant, and Γ is a static stability parameter. The first two forcing terms on the right-hand side (rhs) of (2) are expressed as

[1] As the LOD and GAAM time series are so highly correlated (e.g., Hide et al. 1980; Langley et al. 1981; Rosen and Salstein 1983; Hide and Dickey 1991), the results of this study are found to be essentially insensitive to whether LOD tendency or GAAM tendency is used.

Unauthenticated | Downloaded 05/11/21 11:37 AM UTC

$$F^M = \frac{2\Omega ap}{R\Gamma}\frac{\partial}{\partial\mu}\left[\frac{(1-\mu^2)^{1/2}}{\mu}\frac{\partial F_e}{\partial p}\right];$$

$$F^H = -\Gamma^{-1}\frac{\partial}{\partial\mu}\left[\frac{(1-\mu^2)}{\mu^2}\frac{\partial Q_e}{\partial\mu}\right], \tag{4}$$

where the quantities F_e and Q_e are the eddy momentum and eddy heat fluxes $\overline{u^*v^*}$ and $\overline{v^*T^*}$, respectively, u is zonal wind, v is meridional wind, T is temperature, the overbar denotes a zonal average, and the asterisk the deviation from the zonal average. The remaining two forcing terms on the rhs of (2), D and Q, represent dissipation and diabatic heating, respectively. These terms will be discussed more fully in section 3. The boundary conditions adopted correspond to $v = 0$ at the poles, $\omega = 0$ at $p = 0$, and $D\Phi/Dt = 0$ at the lower boundary $p = p_o = 1000$ mb, where Φ is the geopotential. The variable $\omega(p, \mu)$ is expanded in Hough functions; that is,

$$\omega(p, \mu) = \sum_n \omega_n(p)\Theta_n(\mu), \tag{5}$$

where the $\Theta_n(\mu)$ satisfies the eigenvalue equation

$$\frac{d}{d\mu}\left[\frac{(1-\mu^2)}{\mu^2}\frac{d\Theta_n}{d\mu}\right] - \epsilon_n\Theta_n = 0. \tag{6}$$

The quantities F_e and Q_e are expanded in the associated functions and Hough functions, respectively (see Haynes and Shepherd 1989). Finally, the anomalous mass streamfunction is obtained by the method described above.

3. Results

We first illustrate the contribution of both the friction and mountain torques toward the global angular momentum budget. This is accomplished by regressing both torques and the global relative angular momentum tendency against the LOD tendency (see Fig. 1). The expression for the mountain torque is $T_M(\theta) = -a^2 \cos^2\theta \int_0^{2\pi} p_s(\partial h/\partial x)d\lambda$, where p_s is surface pressure and h is the topographic height. As can be seen, for both seasons, the global anomalous friction torque peaks near lag -6 days and the global anomalous mountain torque near lag $+4$ days. Similar phasing properties have been shown by Hendon (1995), Weickmann et al. (1997), and Feldstein (1999). For the austral winter, the maximum amplitude of the two torques is almost equal, whereas during the boreal winter, the maximum global anomalous mountain torque is about 50% larger than that of the global anomalous friction torque. Figure 1 also shows that the angular momentum budget is reasonably well balanced at all lags between ± 30 days. However, the global relative angular momentum tendency does lag the LOD tendency by about 2 days. The same relationship between relative angular momentum and LOD was found by Weickmann et al. (1997).

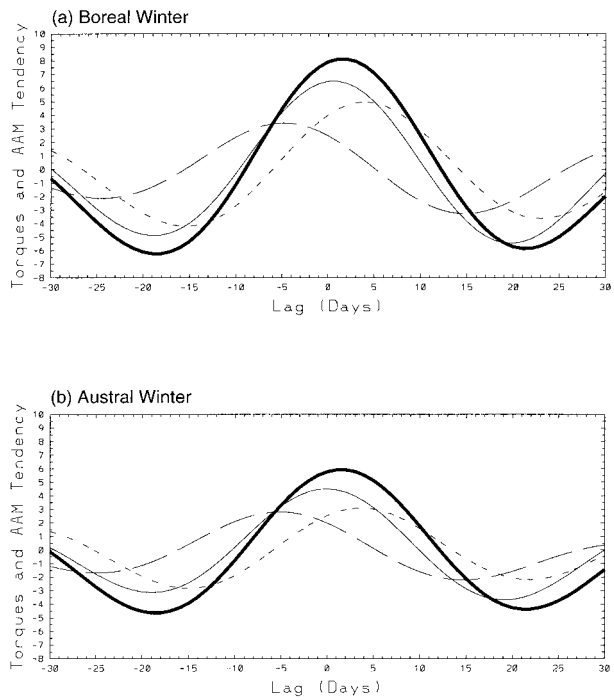

FIG. 1. The anomalous global friction torque (long-dashed line), the anomalous global mountain torque (short-dashed line), the sum of the two global torques (light solid line), and the global relative angular momentum tendency (thick solid line) regressed against the LOD tendency for (a) the boreal winter and (b) the austral winter.

We next examine the anomalous friction torque as a function of latitude and lag (see Fig. 2). The overall features for both seasons are rather similar. For example, the dominant anomalous friction torques occur in the Tropics and subtropics of both hemispheres, and the maximum value occurs in the winter hemisphere. In addition, the maximum winter hemisphere anomalous friction torque leads that of the summer hemisphere by about 3 days.

For each of the calculations presented in sections 3a and 3b, we will focus on lag -6 days relative to the maximum LOD tendency. This particular lag is selected as it corresponds to the lag at which the globally integrated anomalous friction torque is close to its maximum value (Fig. 1). In section 3c, we examine the characteristics of the anomalous MMC driving mechanisms at other lags.

a. Eddy-driven MMC (lag −6 days)

We first compare the anomalous observed (Fig. 3a) and eddy-driven (Fig. 3c) mass streamfunction fields for the boreal winter. [Recall that the eddy-driven mass streamfunction is calculated by solving (2) with D and Q set to zero.] As can be seen, the closest agreement is in the NH Tropics and midlatitudes, where Figs. 3a and 3c both show an anomalous thermally direct cell in the Tropics, and an anomalous thermally indirect cell in the

Unauthenticated | Downloaded 05/11/21 11:37 AM UTC

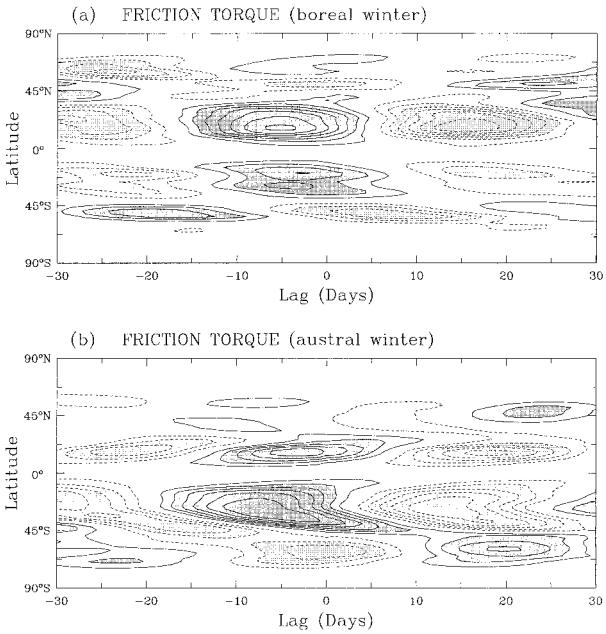

FIG. 2. The anomalous zonal mean friction torque regressed against the LOD tendency. The contour interval is 3.0×10^{17} kg m^2 s^{-2}. Solid contours are positive, dashed contours negative, and the zero contour is omitted. Shading corresponds to values of the anomalous zonal mean friction torque whose magnitude exceeds the second lowest contour line. Dark (light) stippling denoting positive (negative) values.

midlatitudes. However, the amplitude of the two eddy-driven cells is about one-half to one-third that of the corresponding observed cells. Outside this region, the match between the anomalous observed and eddy-driven MMCs is rather poor. For example, the anomalous observed MMC has a cell in the tropical upper troposphere which is absent in anomalous eddy-driven MMC. However, this lack of an upper tropospheric cell in the anomalous eddy-driven MMC is irrelevant for driving a friction torque.

The above analysis considers only the direct impact of the anomalous eddy fluxes on the anomalous MMC. However, as shown from the primitive equation model results of Kim and Lee (2001b), the eddy fluxes can also *indirectly* strengthen the MMC by altering both the diabatic heating and surface friction fields. For example, in regions of anomalous ascending motion, there will be an increase in the diabatic heating that can amplify the already-present anomalous eddy-driven MMC. Furthermore, the anomalous eddy-driven MMC will alter the friction torque, and as Kim and Lee (2001b) show, the adjustment to thermal wind balance results in a further strengthening of the anomalous MMC. Both of these are positive feedback processes. To examine these processes, a very crude parameterization is adopted for the influence of diabatic heating and frictional processes, since daily data for these quantities are not available from the NCEP–NCAR dataset. The aim of these parameterizations is not to accurately determine the anomalous indirect eddy-driven MMC, but to qualitatively assess the magnitude of this process. The procedure adopted simply assumes that the diabatic heating is proportional to the vertical velocity, multiplied by a weighting function that decreases with latitude; that is,

$$Q = \exp[-(\phi/30°)^2]\Gamma\omega(p, \phi). \tag{7}$$

This crude parameterization is based on the scaling property of synoptic-scale systems in the Tropics (see Holton 1992). For the role of frictional processes, we first assume that the frictional force at the lowest model level equals the Coriolis force at that level, and then specify that the frictional force decreases linearly with pressure to a value of zero at 825 mb. When these expressions for the diabatic heating and friction are included on the rhs of the omega equation, that is (2), it is straightforward to solve this equation iteratively. Although both parameterization schemes are obviously very crude, the results (see Fig. 3e) suggest that the effect of both the eddy-driven diabatic heating and the eddy-driven friction is to amplify the anomalous eddy-driven MMC everywhere (calculations performed with either the diabatic heating or friction alone show that the diabatic heating dominates this amplification of the eddy-driven MMC). However, given the fact that these parameterizations are an obvious oversimplification of the true physical processes, it is not useful to state much more.

We next compare the anomalous observed (Fig. 3b) and anomalous eddy-driven (Fig. 3d) mass streamfunction fields for the austral winter. As for the boreal winter, the anomalous observed MMC is dominated by thermally direct cells in the Tropics of either hemisphere. The spatial pattern for the anomalous eddy-driven MMC does show some resemblance to that for the anomalous observed MMC, particularly poleward of about 15°S and 30°N (note that the contour interval in Fig. 3d is one-half that of all the other frames in Fig. 3). However, the maximum amplitude of the anomalous eddy-driven MMC is almost an order of magnitude smaller than that for the anomalous observed MMC. When the diabatic heating and friction parameterizations are included (Fig. 3f), the improvement in the anomalous MMC pattern is rather limited.

The above results suggest that at lag −6 days the eddy-driven MMC plays an important role in driving the anomalous friction torque only during the boreal winter, and primarily in the Northern Hemisphere. At this particular lag, both for the boreal winter Southern Hemisphere (SH) and for both hemispheres during the austral winter, other processes appear to be driving the anomalous MMC, and hence the anomalous friction torque.

As numerous studies have found that the anomalous OLR field associated with the Madden–Julian oscillation (Madden and Julian 1971, 1972) is closely linked to intraseasonal LOD and GAAM variability (e.g., Weickmann et al. 1992; Magana 1993; Weickmann and Sar-

Unauthenticated | Downloaded 05/11/21 11:37 AM UTC

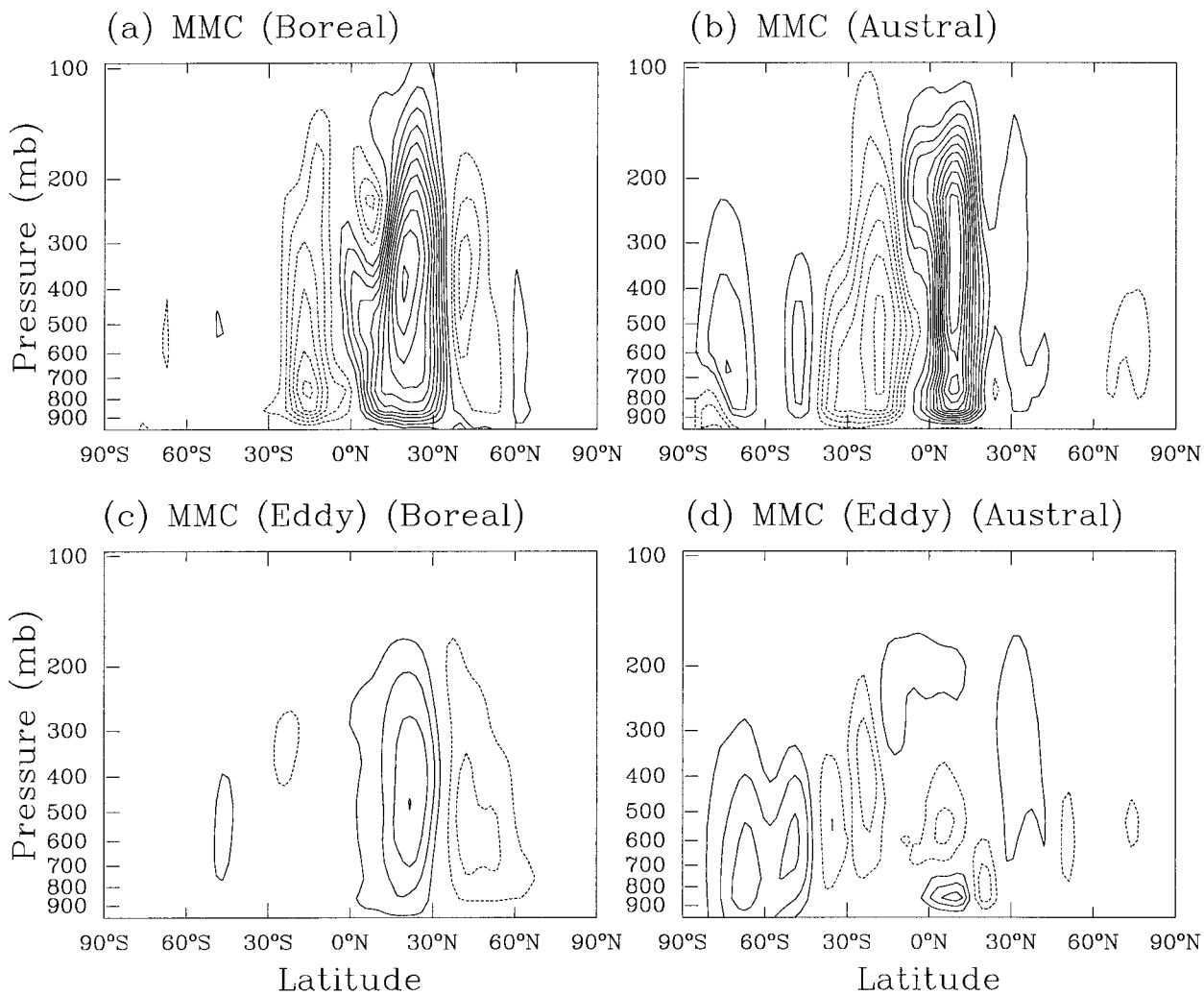

FIG. 3. The anomalous mass streamfunction regressed against the LOD tendency for (a) the boreal winter and (b) the austral winter. The anomalous eddy-driven mass streamfunction for (c) the boreal winter and (d) the austral winter. The anomalous eddy-driven mass streamfunction with parameterized diabatic heating and friction for (e) the boreal winter and (f) the austral winter. All frames corresponds to lag −6 days. The contour interval is 5×10^8 kg s^{-1} for each frame except (d), which has a contour interval of 2.5×10^8 kg s^{-1}. Solid contours are positive, dashed contours negative, and the zero contour is omitted. Solid (dashed) contours indicate a clockwise (counterclockwise) circulation.

deshmukh 1994; Hendon 1995; Feldstein 1999), we also examine the anomalous OLR field at lag −6 days (see Fig. 4). In this figure, negative OLR anomalies correspond to enhanced convection. In order to focus on planetary-scale features, the OLR field is truncated at zonal wavenumber four. Less severe truncations, such as zonal wavenumber seven, are found to yield the same general spatial pattern. As can be seen by comparing Figs. 4a and 4b, the eddy (zonal wavenumbers greater than zero) component of the anomalous OLR field is much stronger during the boreal winter. The anomalous eddy diabatic heating, as represented by the anomalous eddy OLR field in Fig. 4, can excite waves that propagate away from the equator. In fact, consistent with this possibility, for both seasons, the regressed anomalous eddy streamfunction field reveals wave propagation away from the equator (not shown). These waves, through their momentum and heat fluxes, can in turn induce the anomalous MMC. The results in Fig. 4 suggest that at lag −6 days, the boreal winter NH MMC may ultimately be driven by anomalous eddy diabatic heating, via the mechanism described above (in section 3c, results will be presented that suggest that at other lags the SH MMC, during the boreal winter, may also be eddy-driven), and that the austral winter MMC is driven by anomalous zonal mean diabatic heating.

b. Zonal mean tropical convection (lag −6 days)

As discussed in the introduction, anomalous zonal mean diabatic heating associated with convection in Tropics is also expected to drive an anomalous MMC,

Unauthenticated | Downloaded 05/11/21 11:37 AM UTC

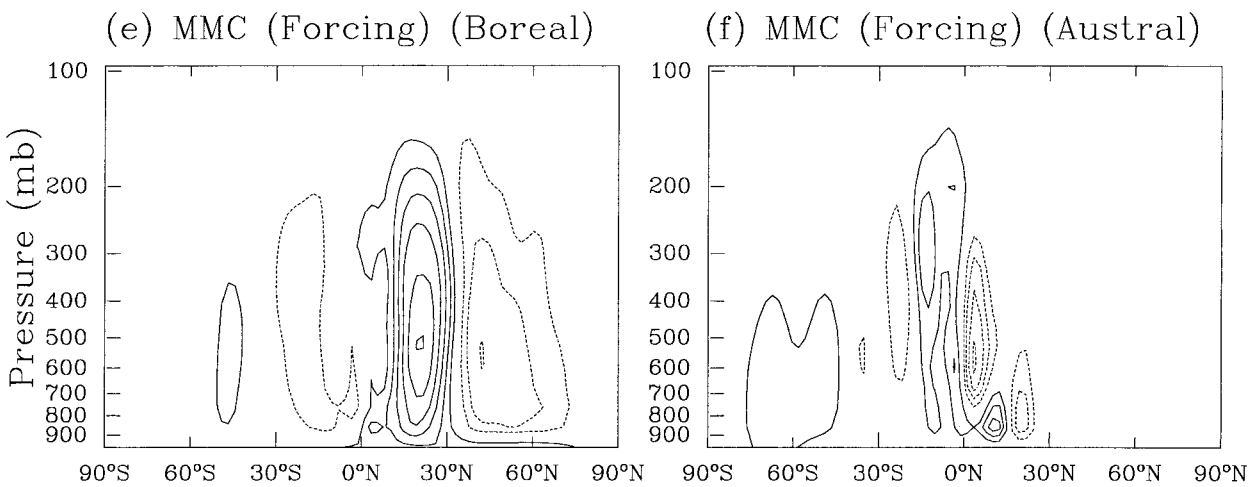

FIG. 3. (*Continued*)

which in turn is capable of driving the anomalous friction torque. By adopting the following procedure, we attempt to estimate the anomalous MMC driven by anomalous zonal mean tropical convection. We take the observed spatial pattern of the anomalous regressed zonal mean OLR field at lag −6 days (see Fig. 5), that is, the time of the maximum anomalous global friction torque, and then generate a timeseries by projecting the daily anomalous zonal mean OLR field onto this spatial pattern. The latitudes selected for this projection extend

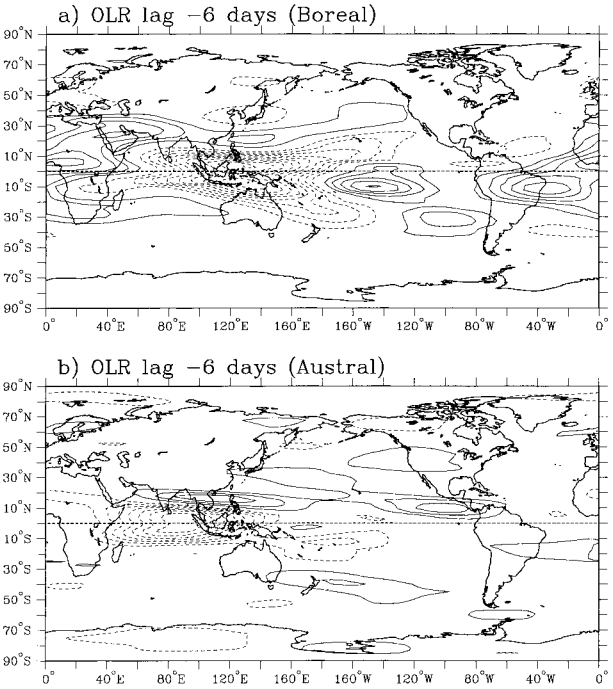

FIG. 4. The anomalous OLR regressed against the LOD tendency at lag −6 days for (a) the boreal winter and (b) the austral winter. The contour interval is 0.6 W m^{-2}. Solid contours are positive, dashed contours negative, and the zero contour is omitted.

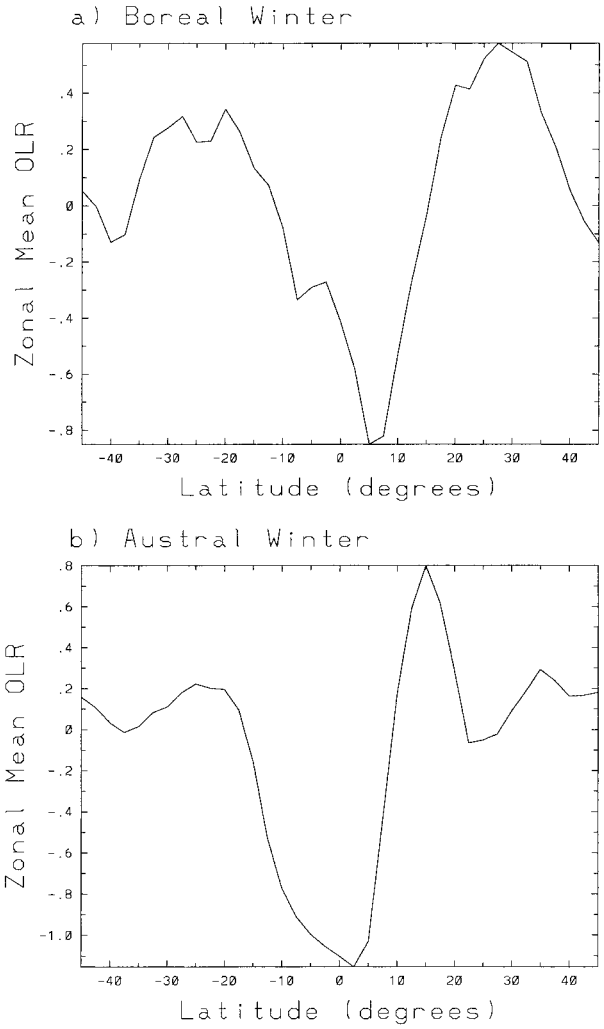

FIG. 5. The anomalous zonal mean OLR regressed against the LOD tendency at lag −6 days for (a) the boreal winter and (b) the austral winter. (Units: W m^{-2}.)

Unauthenticated | Downloaded 05/11/21 11:37 AM UTC

between 45°S and 45°N. The resulting timeseries will be referred to as the zonal mean OLR time series. We then regress the anomalous mass streamfunction field against the zonal mean OLR time series to obtain the associated anomalous MMC field. The MMC obtained in this manner will be referred to as the MMC(OLR) field.

It is important to emphasize that with this approach we are trying to estimate the mass streamfunction response to the anomalous diabatic heating field at lag −6 days. The ideal approach for tackling this problem would be to solve the omega equation, that is, Eq. (2), with Q corresponding to the observed, regressed, bandpass filtered diabatic heating field. However, because the observed daily diabatic heating field is not readily available, the approach described in the above paragraph is adopted. The merit of such an approach can only be tested a posteriori, by comparing the observed anomalous MMC to that obtained by summing the anomalous eddy-driven MMC and the MMC(OLR) fields. It is also important to state that the zonal mean OLR time series must have components that are both coherent and incoherent with the LOD tendency. Because the coherent part of the zonal mean OLR time series must be related to a component of the anomalous MMC that is eddy-driven, it would be preferable to use only the incoherent part, as the regression of the mass streamfunction against the incoherent part of the time series would likely yield a better estimate of the true response to the anomalous zonal mean diabatic heating, independent of the eddy-driving. Because the coherent part of the zonal mean OLR time series is not subtracted, for the boreal winter NH MMC, which includes a strong eddy-driven component, the MMC(OLR) field must include some contribution that is associated with eddy-driving. This concern is unlikely to be relevant for the boreal winter Southern Hemisphere and for both hemispheres of the austral winter at lag −6 days, because the eddy-driven MMC at that lag is feeble.

In order to gain insight into the properties of the MMC(OLR) field, we first examine the seasonal differences in the anomalous zonal mean OLR field (Fig. 5). As can be seen, the anomalous zonal mean OLR field has a similar maximum amplitude during both the boreal and the austral winter. However, for the boreal (austral) winter, the strongest zonal mean convection is located at about 5°N (2°N). Furthermore, the pattern of the austral winter zonal mean convection is somewhat less symmetric about its extrema, as relatively large values of anomalous zonal mean OLR extend into the subtropics of the Southern Hemisphere. An estimate of the latitude that separates equal negative areas under the zonal mean OLR curve between 20°S and 20°N yields a value of about 6°N (2°S) for the boreal (austral) winter. Based on the theoretical findings of Lindzen and Hou (1988), for the boreal winter, these OLR properties suggest that the SH tropical MMC(OLR) field should be much stronger than that in the Northern Hemisphere, and for the austral winter, the NH tropical MMC(OLR) field should be only slightly stronger than that in the Southern Hemisphere. These characteristics are indeed seen in Figs. 6a and 6b.

We next estimate the combined influence of both the eddy driving and the zonal mean tropical convection on the MMC. This is illustrated in Figs. 6c and 6d, which show the sum of the anomalous mass streamfunction fields of Figs. 6a and 3c, and Figs. 6b and 3d, respectively. As can be seen, there is indeed a reasonably good resemblance with the anomalous observed mass streamfunction fields (Figs. 3a and 3b). The biggest discrepancy is found in the boreal winter NH. While the spatial pattern of the sum of the eddy and convectively driven MMC is quite good, its amplitude is too small by about a factor of 2.

c. *Temporal evolution*

While physical processes associated with the friction torque at the time of the maximum LOD tendency (lag −6 days) are of primary interest, more insight into these processes can be gained by examining their temporal evolution. As such, this subsection examines the temporal evolution of the anomalous observed, eddy-driven, and diabatic heating-driven MMCs. The methodologies for estimating the latter two MMCs are described in the previous subsections. Because the mass streamfunction, in general, does not change sign in the vertical direction (e.g., see Figs. 3a and 3b), vertically averaged mass streamfunction, denoted by $\{\psi\}$, will be examined in order to succinctly summarize the anomalous MMC evolution.

1) BOREAL WINTER

The results of section 3a suggest that during the boreal winter the eddies play a large role in driving the anomalous MMC at lag −6 days, particularly for the Northern Hemisphere. In order to investigate whether eddies substantially drive the anomalous MMC at other lags, we examine the observed and eddy-driven $\{\psi\}$ at all lags between ±30 days (see Figs. 7a and 7b). As can be seen, the observed and eddy-driven $\{\psi\}$ fields do have similar spatial patterns at most lags within the Tropics and subtropics, the latitudes for which the anomalous friction torque is largest (Fig. 2). This similarity appears to be much better for the NH. At most lags, the amplitude of the eddy-driven $\{\psi\}$ is only about one-third that of the observed counterpart. When the parameterizations of diabatic heating and surface friction are included, the pattern of the eddy-driven $\{\psi\}$ undergoes very little change, while its amplitude increases by about 80% (not shown).

To quantitatively evaluate the similarity between the patterns in Figs. 7a and 7b, the linear correlation between these two patterns is calculated for all lags between ±30 days and for those latitudes between 45°S

Unauthenticated | Downloaded 05/11/21 11:37 AM UTC

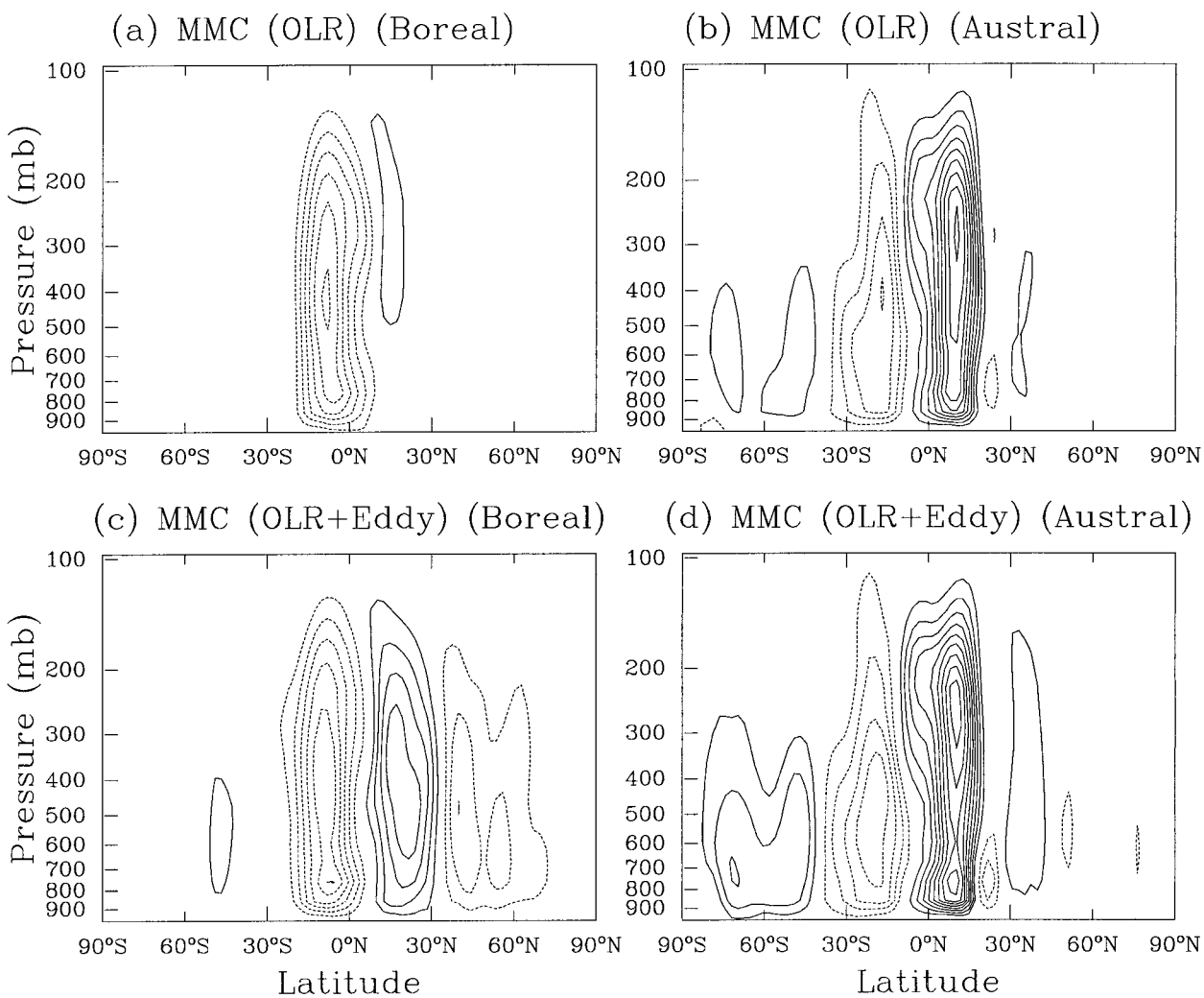

FIG. 6. The anomalous mass streamfunction associated with the zonal mean OLR time series for (a) the boreal winter and (b) the austral winter. The sum of the eddy- and convectively driven anomalous mass streamfunction for (c) the boreal winter and (d) the austral winter. All frames corresponds to lag −6 days. The contour interval is 5×10^8 kg s^{-1}. Solid contours are positive, dashed contours negative, and the zero contour is omitted.

and 45°N. The resulting linear correlation is found to be 0.81 when the parameterized diabatic heating and surface friction are not included, and 0.83 when these parameterizations are taken into account. When these correlations are performed separately for either hemisphere, a value of 0.87 (0.48) is found for the NH (SH). Thus, these results do strongly suggest that the eddies play an important role at all lags in driving the anomalous MMC, particularly for the NH.

A close examination of the phase differences between the observed and eddy-driven $\{\psi\}$ in Figs. 7a and 7b reveals that former lags (leads) the latter by several days in the N(S)H. For the NH, this relationship is consistent with the anomalous observed MMC being primarily eddy-driven, since [as discussed by Plumb (1982)], the adjustment timescale of the MMC is of the order of the inverse of the Coriolis parameter, that is, on the order of 1 day. This implies that for observational data, where the quasigeostrophic constraints[2] do not precisely hold, one should expect the anomalous eddy-driven MMC to lead the anomalous observed MMC, as long as the anomalous observed MMC is primarily eddy-driven. However, the opposite phase relationship for the Southern Hemisphere suggests that eddy forcing is not the dominant mechanism for driving the anomalous MMC.

In order to estimate the temporal evolution of the response of the anomalous MMC to diabatic heating, the zonal mean OLR time series is calculated separately for each lag, following the technique described in the previous subsection. The resulting $\{\psi\}$ field is shown

[2] The instantaneous relationship between forcing and the MMC, as implied by the omega equation, is a requirement of quasigeostrophic theory.

Unauthenticated | Downloaded 05/11/21 11:37 AM UTC

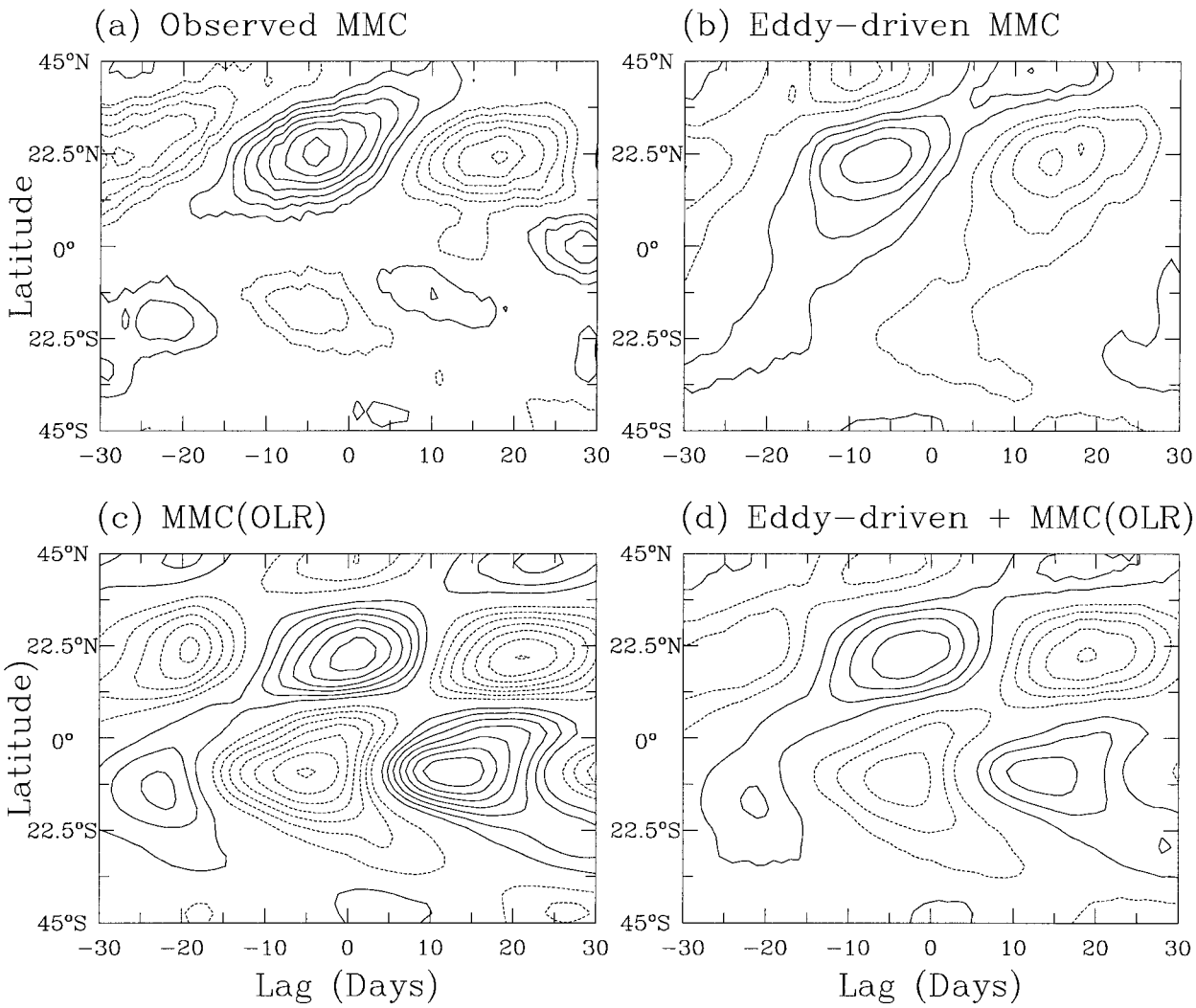

FIG. 7. The boreal winter, vertically averaged mass streamfunction for the (a) anomalous observed MMC, (b) the anomalous eddy-driven MMC, (c) the anomalous MMC(OLR) field, and (d) the sum of (b) and (c). The contour interval is 5×10^8 kg s^{-1} in (a) and (d) and 2.5×10^8 kg s^{-1} in (b) and (c). Solid contours are positive, dashed contours negative, and the zero contour is omitted.

in Fig. 7c. There is a resemblance with the observed $\{\psi\}$ (Fig. 7a), but this similarity is less than that between Figs. 7a and 7b (for the latitude range between 45°S and 45°N, the linear pattern correlation between Figs. 7a and 7c is 0.61). However, when we compare the sum of the eddy-driving and the diabatic heating patterns (see Fig. 7d, which is the sum Figs. 7b and 7c) to the observed pattern in Fig. 7a, the agreement is much better than that between Figs. 7a and 7b, particularly for the SH. (Although the linear spatial correlation between Figs. 7a and 7d is 0.81, the same as between Figs. 7a and 7b, the matching in total amplitude is much improved.)

The above results presented in Fig. 7 suggest that at most lags during the life cycle of LOD variation, both the eddy-driving and the diabatic heating play an important role in driving the anomalous MMC. Furthermore, the similarity between the observed and eddy-driven $\{\psi\}$, and especially the enhancement of this similarity when the parameterizations of the diabatic heating and surface friction are included, suggests that a substantial fraction of the diabatic heating, is in fact, eddy-driven. The relationship between the anomalous OLR field and the anomalous eddy-driven vertical velocity (see Fig. 8) further supports these ideas. In Fig. 8, one noticeable feature is the poleward propagation[3] of both quantities in either hemisphere. Perhaps more interestingly, Fig. 8 shows that in general the eddy-driven upward (downward) motion leads the negative (positive) anomalous zonal mean OLR by a few days. Given the nonzero adjustment timescale for the MMC, as discussed earlier, this feature is consistent with the diabatic heating in both hemispheres being eddy-driven.

[3] During the austral winter, similar propagation of anomalous zonal mean OLR is also found [see Fig. 7 of Feldstein (1999)].

Unauthenticated | Downloaded 05/11/21 11:37 AM UTC

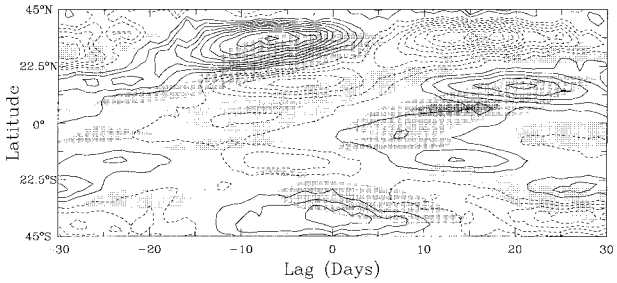

FIG. 8. The anomalous, boreal winter, 500-mb eddy-driven omega (contours) and the anomalous zonal mean OLR (shading). The contour interval is 6×10^{-5} N m^{-2} s^{-1}. Solid contours are positive, dashed contours negative, and the zero contour is omitted. Shaded values exceed a magnitude of 0.3 W m^{-2}, with dark (light) stippling denoting positive (negative) values. The darker enclosed shading for both positive and negative anomalies exceeds a magnitude of 0.75 W m^{-2}.

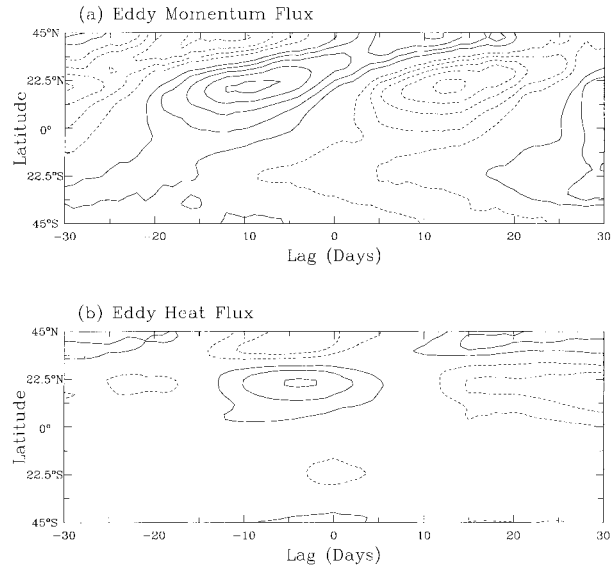

FIG. 9. The anomalous vertically averaged mass streamfunction driven by (a) anomalous eddy momentum fluxes, (b) anomalous eddy heat fluxes during the boreal winter. The contour interval is 1.5×10^8 kg s^{-1} in (a) and (b). Solid contours are positive, dashed contours negative, and the zero contour is omitted.

In addition, because these results show similarities with the solution of the omega equation with a parameterized diabatic heating (see section 3a), and since that solution was characterized by a feedback with the diabatic heating that amplified the MMC, it is plausible that such a feedback is also taking place in the atmosphere during the LOD life cycle. Furthermore, these results also suggest that the poleward zonal mean OLR anomaly propagation, discussed above, must be driven by the eddies.

For the SH, since the anomalous MMC appears not to be eddy-driven (Fig. 7b), and because it is unlikely that the anomalous MMC is driven by zonal mean diabatic heating from the same hemisphere (cf. Figs. 7a and 8), it is plausible that the SH anomalous MMC may be mostly driven by diabatic heating from the NH. Further support for this contention is that the strongest negative anomalous zonal mean OLR occurs in the NH at those lags when $\{\psi\}$ in the SH is largest. As the zonal mean diabatic heating in the NH also appears to be eddy-driven (Fig. 8), we speculate that the anomalous SH MMC may ultimately be driven primarily by the NH eddy fluxes.

The relative contribution of the eddy momentum and heat fluxes toward the driving of the anomalous MMC is summarized in Fig. 9. As can be seen, the NH MMC response to the eddy momentum flux is greater than that for the eddy heat flux. The fact that the timing of the largest individual responses to the two eddy fluxes (lag -9 days for the eddy momentum flux and lag -3 days for the eddy heat flux) straddles that of the largest observed $\{\psi\}$ (lag -5 days, see Fig. 7a), tells us that the anomalous eddy-driven MMC is a response to the driving by both eddy fluxes.

The MMC responses to both the eddy momentum and heat fluxes are also divided into contributions from high-frequency (period <10 days) and low-frequency (period>10 days) transient eddies [for more detail on this division of the fluxes into frequency bands, see Feldstein (1998)]. For the eddy momentum fluxes, the MMC response is found to arise almost entirely from the driving by the low-frequency transient eddies. For the eddy heat fluxes, although the MMC response to the driving from the two frequency bands shows a similar spatial pattern, the amplitude of the MMC response from the low-frequency transient eddies is about three times greater than that from the high-frequency transient eddies. Because low-frequency transient eddies are typically associated with zonally elongated, planetary scale waves (Hoskins et al. 1983), the above results imply that the eddies that drive the MMC are primarily of planetary scale.

2) AUSTRAL WINTER

For the austral winter, when we compare the observed $\{\psi\}$ to that obtained from the zonal mean OLR time series, a strong similarity between these two quantities is found (see Fig. 10; the linear pattern correlation for a latitude range between 45°S and 45°N and for lag ± 30 days is 0.94.) Also, the eddy-driven $\{\psi\}$ (not shown) is found to be much weaker than the observed $\{\psi\}$ at all lags. In addition, the resemblance between the patterns for the eddy-driven and observed $\{\psi\}$ is not very strong (for latitudes between 45°S and 45°N and lag ± 30 days, the pattern correlation is 0.41). Furthermore, the relationship between the anomalous eddy-driven vertical velocity (not shown) and the anomalous zonal mean OLR (not shown) is complex, suggesting that the eddies do not substantially drive the anomalous zonal mean diabatic heating. Thus, these results provide further support that during the austral winter the anomalous MMC is driven primarily by anomalous zonal mean diabatic heating. These findings also suggest that the

Unauthenticated | Downloaded 05/11/21 11:37 AM UTC

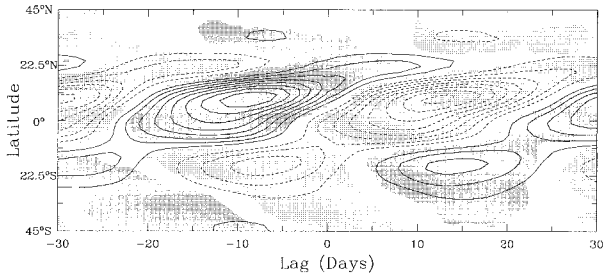

FIG. 10. The austral winter, vertically averaged mass streamfunction. Contours denote the anomalous MMC(OLR) field, and shading denotes the anomalous observed MMC. The contour interval is 4×10^8 kg s^{-1}. Solid contours are positive, dashed contours negative, and the zero contour is omitted. Shaded values exceed a magnitude of 4×10^8 kg s^{-1}, with dark (light) stippling denoting positive (negative) values.

eddy fluxes do not drive the poleward propagation of anomalous zonal mean OLR during the austral winter. [In Feldstein (1999), this propagation is briefly discussed in the context of active and break periods of the Asian summer monsoon.]

4. Conclusions

This study examines the physical processes responsible for driving the anomalous friction torque associated with intraseasonal LOD fluctuations. This is performed by using the anomalous MMC as a proxy for the anomalous friction torque. The key findings are 1) anomalous zonal mean tropical convection appears to be the dominant process in driving the anomalous friction torques in both hemispheres during the austral winter and in the Southern Hemisphere during the boreal winter, and 2) anomalous eddy fluxes appear to drive the anomalous friction torque in the boreal winter NH. The results also suggest that anomalous MMC response to the eddy driving in both hemispheres during the boreal winter is amplified through a positive feedback process which involves a strengthening of the zonal mean diabatic heating by the eddies (Kim and Lee 2001b).

During the boreal winter, in the SH, the dynamics of the anomalous zonal mean convection that drive the anomalous MMC may be rather subtle. This is because anomalous zonal mean diabatic heating from the NH may be driving the SH anomalous MMC, and this particular diabatic heating appears to be excited by the anomalous eddy fluxes, also within the NH. This implies for the boreal winter that the SH anomalous friction torque may also be interpreted as being ultimately driven by eddy fluxes.

It is important to emphasize that the results of this study should be regarded as qualitative. The eddy-driven MMC was obtained from the omega equation, which has inaccuracies associated with the quasi-geostrophic approximation. In addition, in our calculation of the MMC associated with zonal mean tropical convection, it was not possible to entirely distinguish between the eddy-driven and noneddy-driven components. While we anticipate that the qualitative results would remain unchanged, future studies that address these shortcomings would be useful.

Acknowledgments. This research was supported by the National Aeronautics and Space Administration through Grant NAG5-6207. I would like to thank Drs. Sukyoung Lee, Klaus Weickmann, and Harry Hendon for their very beneficial comments on this paper, and Dr. Hyun-kyung Kim for providing me with the computer code for inverting the omega equation. Lastly, I would also like to thank the NOAA Climate Diagnostics Center for providing me with the NCEP–NCAR reanalysis dataset, and Dr. Peter Nelson of Atmospheric and Environmental Research, Inc., for providing me with the LOD time series.

REFERENCES

Dickey, J. O., M. Ghil, and S. L. Marcus, 1991: Extratropical aspects of the 40–50 day oscillation in length-of-day and atmospheric angular momentum. *J. Geophys. Res.,* **96,** 22 643–22 658.

Feldstein, S. B., 1998: An observational study of the intraseasonal poleward propagation of zonal mean flow anomalies. *J. Atmos. Sci.,* **55,** 2516–2529.

——, 1999: The atmospheric dynamics of intraseasonal length-of-day fluctuations during the austral winter. *J. Atmos. Sci.,* **56,** 3043–3058.

Haynes, P. H., and T. G. Shepherd, 1989: The importance of surface pressure changes in the response of the atmosphere to zonally-symmetric thermal and mechanical forcing. *Quart. J. Roy. Meteor. Soc.,* **115,** 1181–1208.

Hendon, H. H., 1995: Length of day changes associated with the Madden–Julian oscillation. *J. Atmos. Sci.,* **52,** 2373–2383.

Hide, R., and J. O. Dickey, 1991: Earth's variable rotation. *Science,* **253,** 629–637.

——, N. T. Birch, L. V. Morrison, D. J. Shea, and A. A. White, 1980: Atmospheric angular momentum fluctuations and changes in the length of day. *Nature,* **286,** 114–117.

Holton, J. R., 1992: *An Introduction to Dynamic Meteorology.* 3d ed. Academic Press, 511 pp.

Hoskins, B. J., I. N. James, and G. H. White, 1983: The shape, propagation, and mean-flow interaction of large-scale weather systems. *J. Atmos. Sci.,* **40,** 1595–1612.

Kim, H.-K., and S. Lee, 2001a: Hadley cell dynamics in a primative equation model. Part I: Axisymmetric flow. *J. Atmos. Sci.,* **58,** 2845–2858.

——, and ——, 2001b: Hadley cell dynamics in a primitive equation model. Part II: Nonaxisymmetric flow. *J. Atmos. Sci.,* **58,** 2859–2871.

Langley, R. B., R. W. King, I. I. Shapiro, R. D. Rosen, and D. A. Salstein, 1981: Atmospheric angular momentum and length of day: A common fluctuation with a period near 50 days. *Nature,* **294,** 730–732.

Lau, K.-M., I.-S. Kang, and P.-J. Sheu, 1989: Principal modes of intraseasonal variations in atmospheric angular momentum and tropical convection. *J. Geophys. Res.,* **94** (D5), 6319–6332.

Lindzen, R. S., and A. Y. Hou, 1988: Hadley circulations for zonally averaged heating centered off the equator. *J. Atmos. Sci.,* **45,** 2416–2427.

Madden, R. A., and P. Julian, 1971: Detection of a 40–50 day oscillation in the zonal wind. *J. Atmos. Sci.,* **28,** 702–708.

——, and ——, 1972: Description of global scale circulation cells in the tropics with a 40–50 day period. *J. Atmos. Sci.,* **29,** 1109–1123.

Unauthenticated | Downloaded 05/11/21 11:37 AM UTC

Magana, V., 1993: The 40- and 50-day oscillations in atmospheric angular momentum at various latitudes. *J. Geophys. Res.,* **98,** 10 441–10 450.

Peixoto, J. P., and A. H. Oort, 1992: *Physics of Climate.* American Institute of Physics, 520 pp.

Plumb, R. A., 1982: Zonally symmetric Hough modes and meridional circulations in the middle atmosphere. *J. Atmos. Sci.,* **39,** 983–991.

Rosen, R. D., and D. A. Salstein, 1983: Variations in atmospheric angular momentum on global and regional scales and length of day. *J. Geophys. Res.,* **88,** 5451–5470.

Weickmann, K. M., and P. D. Sardeshmukh, 1994: The atmospheric angular momentum cycle associated with a Madden–Julian oscillation. *J. Atmos. Sci.,* **51,** 3194–3208.

——, S. J. S. Khalsa, and J. Eischeid, 1992: The atmospheric angular-momentum cycle during the tropical Madden–Julian oscillation. *Mon. Wea. Rev.,* **120,** 2252–2263.

——, G. N. Kiladis, and P. D. Sardeshmukh, 1997: The dynamics of intraseasonal atmospheric angular momentum oscillations. *J. Atmos. Sci.,* **54,** 1445–1461.

Unauthenticated | Downloaded 05/11/21 11:37 AM UTC